Received: 5 July 2019 | Revised: 23 October 2019 | Accepted: 24 October 2019

DOI: 10.1002/psc.3233

RESEARCH ARTICLE

WILEY Journal of PeptideScience

# Structure-activity relationship studies of shortened analogues of the antimicrobial peptide EeCentrocin 1 from the sea urchin *Echinus esculentus*

Runar G. Solstad[1,2] | Cecilie Johansen[3] | Klara Stensvåg[1] | Morten B. Strøm[3] | Tor Haug[1]

[1] The Norwegian College of Fishery Science, Faculty of Biosciences, Fisheries and Economics, UiT - The Arctic University of Norway, Tromsø, Norway

[2] Nofima – The Norwegian Institute of Food, Fisheries and Aquaculture Research, Tromsø, Norway

[3] Department of Pharmacy, Faculty of Health Sciences, UiT - The Arctic University of Norway, Tromsø, Norway

**Correspondence**
Tor Haug, The Norwegian College of Fishery Science, Faculty of Biosciences, Fisheries and Economics, UiT - The Arctic University of Norway, Tromsø, Norway.
Email: tor.haug@uit.no

**Funding information**
Norges Forskningsråd, Grant/Award Number: 208546; Research Council of Norway; XBioPepS, Grant/Award Number: 208546

EeCentrocin 1 is a potent antimicrobial peptide isolated from the marine sea urchin *Echinus esculentus*. The peptide has a hetero-dimeric structure with the antimicrobial activity confined in its largest monomer, the heavy chain (HC), encompassing 30 amino acid residues. The aim of the present study was to develop a shorter drug lead peptide using the heavy chain of EeCentrocin 1 as a starting scaffold and to perform a structure-activity relationship study with sequence modifications to optimize antimicrobial activity. The experiments consisted of 1) truncation of the heavy chain, 2) replacement of amino acids unfavourable for *in vitro* antimicrobial activity, and 3) an alanine scan experiment on the truncated and modified heavy chain sequence to identify essential residues for antimicrobial activity. The heavy chain of EeCentrocin 1 was truncated to less than half its initial size, retaining most of its original antimicrobial activity. The truncated and optimized lead peptide (**P6**) consisted of the 12 *N*-terminal amino acid residues from the original EeCentrocin 1 HC sequence and was modified by two amino acid replacements and a *C*-terminal amidation. Results from the alanine scan indicated that the generated lead peptide (**P6**) contained the optimal sequence for antibacterial activity, in which none of the alanine scan peptides could surpass its antimicrobial activity. The lead peptide (**P6**) was also superior in antifungal activity compared to the other peptides prepared and showed minimal inhibitory concentrations (MICs) in the low micromolar range. In addition, the lead peptide (**P6**) displayed minor haemolytic and no cytotoxic activity, making it a promising lead for further antimicrobial drug development.

KEYWORDS

SAR-study, structure-activity relationship study, EeCentrocin 1, *Echinus esculentus*, antimicrobial peptide, truncation

**Abbreviations:** AMPs, Antimicrobial peptides; HC, The heavy chain of the heterodimeric peptide EeCentrocin 1; LC, The light chain of the heterodimeric peptide EeCentrocin 1; MIC, Minimum inhibitory concentration; Cg, *Corynebacterium glutamicum*; Sa, *Staphylococcus aureus*; Pa, *Pseudomonas aeruginosa*; Ec, *Escherichia coli*

## 1 | INTRODUCTION

Bacterial resistance to commercial antibiotics has increased severely over the last years. Infectious bacteria that were once easily treatable by antibiotics have now become resistant.[1] There is consequently a pressing need to come up with alternatives to the current antimicrobial drugs. Antimicrobial peptides (AMPs) are proteinaceous natural products found in all living phyla examined, and due to their high structural diversity, they are considered attractive hit compounds for development of drug leads for novel antibiotics. AMPs efficiently kill bacterial pathogens with low toxicity to mammalian cells, and often have broad-spectrum antimicrobial activity against pathogenic Gram-positive and Gram-negative bacteria.[2-4] Most AMPs appear to interact with bacterial membranes, forming pores or aggregates at the membrane surface, causing cooperative permeabilization and loss of membrane integrity.[3] In membrane-like environments, AMPs tend to form amphipathic structures, i.e. structures with separate hydrophobic and hydrophilic domains. Their net positive charge facilitates interactions with the negatively charged bacterial membranes and/or cell walls, whereas their amphipathic character enables membrane permeabilization.[4] Because AMPs in general act on the lipid bilayer structure of bacterial membranes, there seems to be lower propensity of generating resistance against AMPs compared to other antibiotic classes.[5-7] There is even recent evidence that antibiotic-resistant *Escherichia coli* display increased sensitivity towards AMPs.[8] Some AMPs have additional mode of actions, attacking both extracellular and intracellular targets rapidly.[8,9] Several AMPs are currently in the medical pipeline due to these favourable properties.[10-13]

The centrocins are potent marine natural AMPs originally isolated and characterised from the sea urchins *Strongylocentrotus droebachiensis*[14] and *Echinus esculentus*.[15] Centrocin-coding genes have also been identified in the genome of *S. purpuratus*.[16] The centrocins display antimicrobial activities in the sub-micromolar range against both Gram-positive and Gram-negative bacteria, as well as fungi. Centrocins range from 4.4-4.8 kDa in size and have a heterodimeric structure, i.e., they have a heavy chain (HC) of ~30 amino acid residues which is linked by a disulphide bridge to a light chain (LC) of ~12 amino acid residues. All isolated centrocins contain brominated tryptophan residues in their HC. Previous *in vitro* experiments have shown that the antimicrobial activity is confined to the HC's and that non-brominated HC peptides are equally potent as the brominated ones. These data imply other purposes than direct involvement in bacterial killing for the LC and the brominated tryptophan residues.[14,15]

In the present study, we aimed to design a shorter AMP with improved or similar antimicrobial activity as the non-brominated HC of EeCentrocin 1 derived from *E. esculentus*.[15] This was done by successive structure-activity relationship (SAR) studies - concentrated on truncation, sequence modification, *C*-terminal amidation, and alanine scanning. The EeCentrocin 1 HC was chosen as a framework because of its potent antibacterial activity and low haemolytic activity.[15] The hypothesis was that the bioactive part of EeCentrocin 1 HC could be attributed to the *N*-terminal region, which contain both hydrophobic tryptophan residues and cationic residues - two structural properties known to contribute to antimicrobial activity in other AMPs.[17-19]

## 2 | MATERIALS AND METHODS

### 2.1 | Solid phase peptide synthesis (SPPS)

The non-brominated HC of EeCentrocin 1 (**P1**), the truncated peptide HC(1-16) (**P2**), and the modified peptide HC(1-16)A8 (**P3**) were acquired commercially (GenicBio Ltd., Shanghai, China). The other peptides (**P4-P18**) were synthesized in-house by microwave assisted Fmoc solid-phase peptide synthesis (Fmoc-SPPS). All Fmoc-amino acids and solvents were purchased from Sigma-Aldrich (MO, USA), whereas Rink amide ChemMatrix resin was obtained from Biotage (Uppsala, Sweden). The most efficient procedure involved using Rink amide ChemMatrix resin (loading 0.47-0.49 mmol/gram), which was swelled in *N*,*N*-dimethylformamide (DMF) in a 10 mL fritted reaction vial for 20 min with microwave heating at 70°C. Fmoc-amino acids (4.2 eq.) were dissolved in N-methyl-2-pyrrolidone (NMP) prior to *in situ* coupling with O-(6-chlorobenzotriazol-1-yl)-*N*,*N*,*N*′,*N*′-tetramethyluronium hexafluorophosphate (HCTU, 4.2 eq.) and *N*,*N*-diisopropylethylamine (DIEA, 8.4 eq.) as base, and coupling for five min with microwave heating at 75°C. Fmoc-Arg (Pbf)-OH was coupled at room temperature for 60 min to avoid δ-lactamisation of its side-chain, and we found it necessary to double couple the *N*-terminal Gly-residue to avoid Gly-1 deletion peptides. Fmoc-cleavage was performed with a solution of 20% piperidine in DMF (4.5 mL for three min and repeated for 10 min) at room temperature, and the resin washed with DMF (4 × 4.5 mL for 0.45 min). After the final coupling and Fmoc-cleavage of the *N*-terminal residue, the resin was washed thoroughly with dichloromethane (DCM) and dried overnight in a desiccator. A 10 mL solution of 95% trifluoroacetic acid (TFA), 2.5% triisopropylsilane (TIS), and 2.5% $H_2O$ was used as cleavage cocktail and added to the 10 mL fritted reaction vial with gentle stirring every hour for 3-3.5 h. The solution was filtered on a Supelco Visiprep vacuum manifold and the cleavage process was repeated with 5 mL of the cleavage cocktail for 0.5-1 h. The solution was concentrated *in vacuo* and ice-cold diethyl ether was added for precipitation of the crude peptide. The precipitated crude peptide was washed three times with ice-cold diethyl ether to remove traces of the cleavage cocktail.

### 2.2 | Purification and characterization

The peptides (**P4-P18**) were purified by preparative RP-HPLC using a Waters 2690 separation module equipped with a Waters 996 photodiode array detector and an XBridge $C_{18}$, 5 µm, 10 × 250 mm column (Waters, MA USA). The mobile phases consisted of eluent A: deionized $H_2O$ and eluent B: 95% acetonitrile (ACN)/5% $H_2O$, both containing 0.1% TFA. Depending on the individual peptide (hydrophobicity and co-eluting reagents), linear gradients for purification went from 5-17% of eluent B to 35% eluent B in 24 min at a flow of 5 mL/min. The purity of all peptides was calculated to be above 95%, as

determined by UV-absorbance at 214 nm. Molecular mass and purity of the peptides were confirmed using a high-resolution 6540B Q-TOF mass spectrometer with a dual ESI source, coupled to a 1290 Infinity UHPLC system, controlled by the MassHunter software (Agilent, CA, USA). The peptides were separated using a Zorbax C18, 2.1×50 mm, 1.8 µm column (Agilent). System details and typical parameters are found in the supporting information (S1 table). The mobile phase consisted of $H_2O$ and ACN, both containing 0.1% formic acid, and a linear gradient of 5-60% ACN at a flow rate of 0.4 mL/min was used during the LC-MS analysis. The measured masses of all peptides were within 10 ppm of their theoretical values. A specific gradient running from 3-20% ACN was applied for the determination of peptide hydrophobicity, i.e. retention times on a reversed-phase C18 column.

## 2.3 | Antimicrobial susceptibility testing

### 2.3.1 | Antibacterial assay

The peptides were screened for antibacterial activity against two strains of Gram-positive and two strains of Gram-negative bacteria; *Corynebacterium glutamicum* (Cg, ATCC 13032), *Staphylococcus aureus* (Sa, ATCC 9144), *Pseudomonas aeruginosa* (Pa, ATCC 27853), and *E. coli* (Ec, ATCC 25922). Cultures stored at -80°C in glycerol were transferred to Mueller-Hinton plates (MH, Difco, Lawrence, KS, USA) and incubated for 24 h at 35°C. A few colonies of each bacterial strain were transferred to 5 mL liquid MH medium and left shaking (600 rpm) at room temperature overnight. Cultures of actively growing bacteria (20 µL) were inoculated in 5 mL MH medium and left shaking for 2 h at room temperature. The antibacterial assays were performed as previously described by Sperstad and co-workers[20] with the following exception: bacterial cultures were diluted with medium to 2.5-3 × $10^4$ cells/mL concentrations. An aliquot of 50 µL (1250-1500 bacterial cells) was added to each well in 96-well Nunclon™ microtiter plates (Nagle Nunc Int., Denmark) preloaded with peptide solution (50 µL). The microtiter plates were incubated for 24 h at 35°C with optical density recorded every hour using an Envision 2103 multilabel reader, controlled by a Wallac Envision manager (PerkinElmer, CT, USA). Minimum inhibitory concentration (MIC) was defined as a sample showing complete inhibition (as measured by optical density at 595 nm) compared to the negative (growth) controls, consisting of bacteria and water. Oxytetracycline hydrochloride (20 µM, Sigma-Aldrich) served as a positive (inhibition) control. The synthetic peptides were tested for antibacterial activity in concentrations ranging from 200 to 0.1 µM in two-fold dilutions. All tests were performed in triplicates.

A killing experiment was performed on HC(1-12)A8K12 (**P6**). Actively growing cultures of *S. aureus* (ATCC 9144) and *E. coli* (ATCC 25922) were diluted in MH broth to a concentration of 2.5-3 × $10^4$ cells/mL and incubated in 96-well Nunclon™ microtiter plates (Nagle Nunc) at 37°C in the absence/presence (0−50 µM) of the antimicrobial peptide, as described above. Optical density (595 nm) was recorded every hour using an Envision 2103 multilabel reader (PerkinElmer). After 24 h of treatment, aliquots (10 µL) of 10-fold serial dilutions (in MH broth) of wells containing MIC, ½ × MIC, and ¼ × MIC of the peptide were plated on MH Agar (Difco) plates. The number of colony-forming units (CFU) was determined after 24 h of incubation at 37°C. Both tests were performed in triplicates.

### 2.3.2 | Antifungal assay

The synthetic peptides were also screened for antifungal activity against *Candida albicans* (ATCC 10231), *Aureobasidium pullulans*, and *Rhodotorula* sp. (the last two were obtained from Professor Arne Tronsmo, The Norwegian University of Life Sciences, Ås, Norway). The antifungal assay was performed as previously described.[21] Briefly, fungal spores were dissolved in potato dextrose broth (Difco) to a concentration of 4 × $10^5$ spores/mL. The spores (50 µL) were inoculated on 96-well Nunclon™ microtiter plates containing the synthetic peptides (50 µL) dissolved in MQ-$H_2O$. MIC, defined as the lowest concentration of peptide giving no visible growth, was determined visually after incubation for 24 h at room temperature. The negative (growth) control consisted of medium and fungal solution, whereas fluconazole (Sigma-Aldrich) served as positive antifungal control. The peptides and fluconazole were tested for activity in concentrations ranging from 100 to 0.1 µM in two-fold serial dilutions. All tests were performed in triplicates.

### 2.3.3 | Haemolytic assay

The synthesised peptide analogues were screened for eukaryotic cell-toxicity with a haemolytic activity assay using human red blood cells (RBC) as described previously.[21] The assay was performed in 96-well U-shaped microtiter plates (Nagle Nunc) with 50 µL peptide sample, 40 µL phosphate-buffered saline (PBS) and 10 µL red blood cells. After one hour of incubation at 37°C in a shaker, the plate was centrifuged at 200 g for 5 min and the supernatants (60 µL) were carefully transferred to a new flat-bottomed polycarbonate microtiter plate (Nagle Nunc) and the release of haemoglobin (absorbance at 550 nm) was measured on a Synergy H1 multimode reader (BioTek, VT, USA). Cell suspension added 0.05% Triton X-100 (Sigma-Aldrich) in PBS served as positive (100% haemolysis) control and cell suspension added PBS served as negative (0% haemolysis, blank) control. The percent haemolysis was calculated using the formula [(sample-baseline)/(triton-baseline)]×100. The cytotoxic peptide melittin (Sigma-Aldrich) was used as a positive control peptide and for comparison. The experiment was performed in triplicates with peptide concentrations ranging from 200 µM to 1.56 µM in twofold serial dilutions.

### 2.3.4 | Cytotoxicity assay

The peptides were screened for cytotoxic activity in 96-well plates against two adherent cell lines; human melanoma cells (A2058, ATCC CRL-1114, Manassas, VA, USA) and non-malignant human lung fibroblasts (MRC-5, ATCC CCL-171). Cell viability was determined using a colorimetric 3-(4,5-dimethylthiazol-2-yl)-5-(3-carboxymethoxyphenyl)-2-(4-sulfophenyl)-2H-tetrazolium (MTS) assay,[22] with minor

modifications. Cells assayed with their respective cell media served as negative control, whereas cells assayed with 10% DMSO served as positive control. Cell viability was calculated as follows: Cell survival (%) = (absorbance treated wells − absorbance positive control)/(absorbance negative control − absorbance positive control) × 100. All tests were performed in triplicates, using peptide concentrations from 200 μM to 6.25 μM in twofold serial dilutions.

### 2.4 | Bioinformatics

Peptide properties were calculated with PEPCALC (http://pepcalc.com) from Innovagen AB, and helical wheel projections made with Pepwheel at the EMBOSS suite (http://www.bioinformatics.nl/cgi-bin/emboss/pepwheel). Secondary structures were predicted using the PROTEUS Structure Prediction Server 2.0 (http://www.proteus2.ca/proteus2/index.jsp)[23] and PEP-FOLD3 (http://bioserv.rpbs.univ-paris-diderot.fr/services/PEP-FOLD3/),[24] and resulting figures were made with BIOVIA Discovery Studio Visualizer v4.5.0.15071 (Dassault Systèmes, San Diego). Homology searches for non-redundant protein sequences were performed with the Basic Local Alignment Search Tool (BLAST) provided by the National Centre for Biotechnological Information (NCBI) server (http://blast.ncbi.nlm.nih.gov/Blast.cgi).[25]

## 3 | RESULTS AND DISCUSSION

In the present study, a series of shortened peptides, based on the marine heterodimeric and brominated AMP EeCentrocin 1 (originally isolated from the red sea urchin *E. esculentus*), were chemically synthesized and screened for antimicrobial activity. Initial experiments involved the stepwise truncation of the non-brominated HC of the peptide. The LC and bromination of the Trp-residues within the HC were excluded from this study because of their minor importance for antimicrobial activity.[15]

### 3.1 | Truncation of non-brominated HC

*In silico* modelling of the EeCentrocin 1 HC (**P1**, Figure 1) revealed that the *N*-terminal part of the sequence most likely forms an α-helix, a well-known conformation of AMPs. The *N*-terminal has an abundance of hydrophobic and cationic residues, which is a characteristic known to be of importance for the activity of AMPs.[19] Furthermore, the *N*-terminal region of many α-helical AMPs is shown to be important for antimicrobial activity.[17] Based on this qualified sequence evaluation of the HC of EeCentrocin 1, the last 14 *C*-terminal amino acid residues were removed, resulting in the peptide HC(1-16) (**P2**, Table 1). The peptide contains two Trp and six cationic residues (Arg/Lys). Truncation of the heavy chain led to reduced antibacterial activity, especially against *S. aureus*. However, the Gram-positive *C. glutamicum* was still sensitive to **P2** albeit at a slightly higher concentration. An eight-fold decrease in potency was also observed against the Gram-negative test bacteria, maybe due to reduced charge of **P2** compared to the full HC peptide (Table 1).

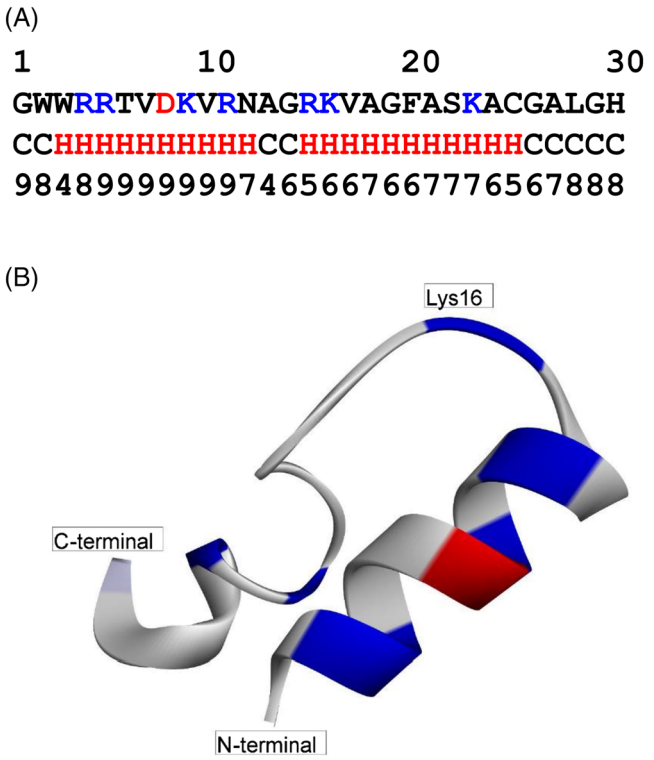


**FIGURE 1** *In silico* secondary structure prediction of the 30 residues long EeCentrocin 1 HC (**P1**). Secondary structure predicted by the Proteus Structure Prediction Server (A). Line 1 shows the amino acid sequence of EeCentrocin 1 HC, with cationic residues in blue and the anionic residue in red. Line 2 indicates type of secondary structure (H = helix, C = coil). Line 3 indicates confidence score of the prediction (0-9, 0 = low, 9 = high). Secondary structure predicted by the PEP-FOLD3 software and visualized using the BIOVIA software (B)

Since an electrostatic interaction between cationic AMPs and the negatively charged surface of bacteria is important for antibacterial activity,[26] the negatively charged Asp8 residue was replaced by an Ala-residue and the *C*-terminal Lys-residue amidated in HC(1-16)A8 (**P3**). **P3** was antibacterial at low concentrations and clearly pointed to the importance of increasing the overall positive charge of the peptide (Table 1). Thus, all subsequent synthesised AMPs were prepared with the Asp8 residue substituted with Ala (or Arg) as well as having a *C*-terminal amide. Carboxyamidation, which increases the overall positive charge of the peptides, is previously shown to increase the antimicrobial activity of AMPs.[27]

Early in the process, it was discovered that eliminating the *N*-terminal Gly1 was not beneficial for antibacterial activity as shown for the resulting peptide HC(2-16)A7 (**P4**). **P4** displayed a remarkable drop in antibacterial activity against the Gram-negative *P. aeruginosa* compared to the HC(1-16)A8 (**P3**) analogue (Table 1). However, the activity against the other test strains remained the same. The importance of Gly1 has been discussed before – the presence of an *N*-terminal Gly-residue was recorded in 70% of 150 α-helical AMPs collected from the AMSDb database, perhaps serving as a capping residue for α-helices or providing resistance to aminopeptidases.[17]

As the *N*-terminal truncation proved unsuccessful against *P. aeruginosa*, the focus was directed towards further truncation of the

**TABLE 1** Sequences and *in vitro* antibacterial activities (MIC, μM) of the heavy chain (HC) of EeCentrocin 1 (**P1**) and HC truncated and modified analogues (**P2-P7**). The table also shows in-text number reference for each peptide, molecular weight (MW, g/mol), and peptide net charge

| | | | Amino acid sequence and position | | | | | | | | | | | | | | | | | | | | | | | | | | MIC (μM) | | | |
|---|---|---|---|---|---|---|---|---|---|---|---|---|---|---|---|---|---|---|---|---|---|---|---|---|---|---|---|---|---|---|---|---|
| No. | Peptide | MW | 1 | 2 | 3 | 4 | 5 | 6 | 7 | 8 | 9 | 10 | 11 | 12 | 13 | 14 | 15 | 16 | 17 | 18 | 19 | 20 | 21 | 22 | 23 | 24 | 25 | 26 | 27 | 28 | 29 | 30 | C-term | Charge | Cg | Sa | Pa | Ec |
| P1 | HC[1] | 3255.7 | G | W | W | R | R | T | V | D | K | V | R | N | A | G | R | K | V | A | G | F | A | S | K | A | C | G | A | L | G | H | -OH | +6 | 0.4 | 3.1 | 1.6 | 0.8 |
| P2 | HC(1-16) | 1985.3 | G | W | W | R | R | T | V | D | K | V | R | N | A | G | R | K | | | | | | | | | | | | | | | -OH | +5 | 0.8 | 200 | 12.5 | 6.3 |
| P3 | HC(1-16)A8 | 1940.3 | G | W | W | R | R | T | V | A | K | V | R | N | A | G | R | K | | | | | | | | | | | | | | | $-NH_2$ | +7 | 0.8 | 12.5 | 3.1 | 3.1 |
| P4 | HC(2-16)A7 | 1883.2 | | W | W | R | R | T | V | A | K | V | R | N | A | G | R | K | | | | | | | | | | | | | | | $-NH_2$ | +7 | 0.4 | 12.5 | 25 | 6.3 |
| P5 | HC(1-12)A8 | 1527.8 | G | W | W | R | R | T | V | A | K | V | R | N | | | | | | | | | | | | | | | | | | | $-NH_2$ | +5 | 1.6 | 50 | 6.3 | 6.3 |
| P6 | HC(1-12)A8K12 | 1541.9 | G | W | W | R | R | T | V | A | K | V | R | K | | | | | | | | | | | | | | | | | | | $-NH_2$ | +6 | 0.4 | 12.5 | 1.6 | 3.1 |
| P7 | HC(1-9)R8 | 1243.5 | G | W | W | R | R | T | V | R | K | | | | | | | | | | | | | | | | | | | | | | $-NH_2$ | +5 | 3.1 | 100 | 25 | 50 |

[1]Antibacterial data of EeCentrocin 1 HC (**P1**) are derived from Solstad *et al*.[15]

*C*-terminal end, resulting in the peptide HC(1-12)A8 (**P5**). The antibacterial activity of **P5** was somewhat reduced compared to the larger HC(1-16)A8 (**P3**) against all strains (Table 1). To improve the antibacterial activity of this 12-residue peptide, the *C*-terminal Arg-Lys-motif, which was recognised in the 16-residue peptides, was reinstated. This also made it possible to replace the original Asn12-residue, which can compromise peptide integrity by forming aspartimide side-products in SPPS involving chain-elongation through its side-chain and not the peptide-backbone.[28] The resulting peptide HC(1-12)A8K12 (**P6**) was the most potent AMP produced so far with antibacterial activities towards *C. glutamicum* and *P. aeruginosa* close to the original HC (**P1**) peptide (Table 1).

The next analogue HC(1-9)R8 (**P7**) was synthesised using the same argument as with HC(1-12)A8 (**P3**) and HC(1-12)A8K12 (**P6**) to further shorten the peptide sequence and reinstate the *C*-terminal Arg-Lys-motif. However, the potency of this 9-residue peptide (**P7**) was much lower than the previous peptides, maybe due to reduction in net positive charge (Table 1).

Accordingly, HC(1-12)A8K12 (**P6**) became our lead peptide after the truncation experiments and represented an AMP 2/5 the sequence-size of the original HC (**P1**). **P6** contains 5 positively charged residues and an amidated *C*-terminus resulting in a net charge of +6 (Table 1, Figure 2A). The 12-residue lead peptide was predicted to form an α-helical structure (Figure 2B), similar to what was predicted for the *N*-terminal part of EeCentrocin 1 HC (**P1**) (Figure 1). Compared to the original HC (**P1**) of EeCentrocin 1 and homologues in *S. droebachiensis* and *S. purpuratus*, the *N*-terminal regions have similar physiochemical properties (Table 2); all having a conserved Trp2, a bulky aromatic residue in position 3, charged residues in positions 5 and 8, and a conserved Val10. These similarities might indicate that these residues are important for antimicrobial activity. The lead peptide HC(1-12)A8K12 (**P6**) differs in position 8 with insertion of a small hydrophobic residue (Ala8) instead of a charged residue.

## 3.2 | Alanine-scan of the lead peptide HC(1-12)A8K12

In order to investigate the importance to antibacterial activity of individual residues of the lead peptide HC(1-12)A8K12 (**P6**), each amino acid was substituted by Ala and antibacterial activity was recorded for each peptide in an alanine scan. Ala, along with Leu and Lys are known stabilisers of peptide α-helicity.[29] The peptides were named (apart from the lead peptide, **P6**) according to the original amino acid, position and substitution, i.e. the peptide where Gly was substituted with Ala in position 1, was named G1A. All Ala-scan peptides displayed antibacterial activity, but with different potencies against different strains (Table 3). Overall, *C. glutamicum* was the most sensitive strain when treated with peptides. The other Gram-positive strain, *S. aureus*, was the least sensitive strain in the current experiment, resisting all the AMPs at concentrations below 12.5 μM. Only four AMPs were antibacterial against *S. aureus* at concentrations ≤25 μM; the lead peptide HC(1-12)A8K12 (**P6**), G1A (**P8**), W3A (**P10**) and T6A (**P13**),

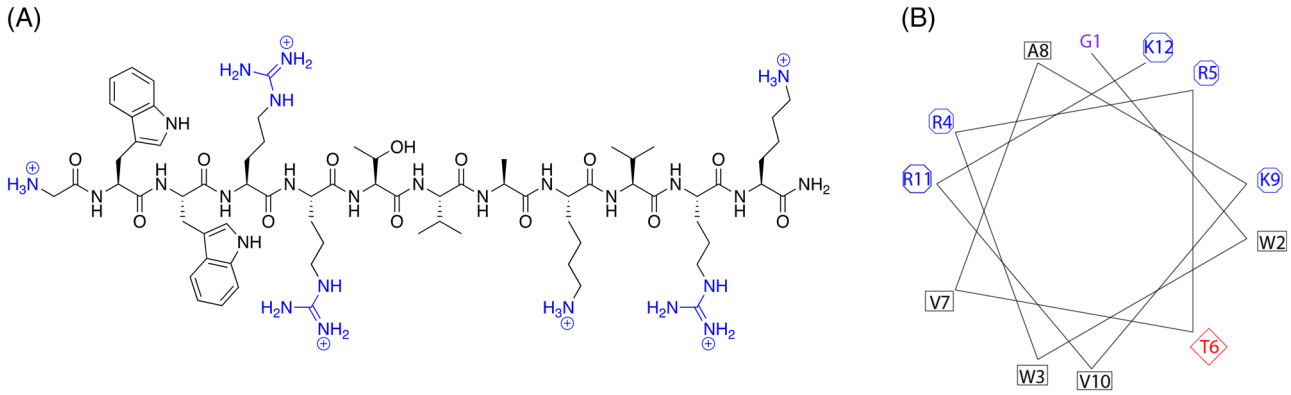


**FIGURE 2** Chemical structure (A) and helical wheel projection (B) of the lead peptide HC(1-12)A8K12 (**P6**). Cationic residues are highlighted in blue. Black boxes in the helical wheel signify hydrophobic residues, whereas the polar Thr6 residue (T6) in the hydrophobic face of the predicted α-helix is depicted with a red diamond

**TABLE 2** Alignment of the 12-residue lead peptide HC(1-12)A8K12 (**P6**) with the *N*-terminal region (residues 1-12) of EeCentrocin 1 HC (**P1**), SdCentrocin 1a HC and 2 HC from *S. droebachiensis*, and putative centrocin HCs from *S. purpuratus*.

| | | Amino acid sequence and amino acid position | | | | | | | | | | | |
|---|---|---|---|---|---|---|---|---|---|---|---|---|---|
| Peptide | Origin | 1 | 2 | 3 | 4 | 5 | 6 | 7 | 8 | 9 | 10 | 11 | 12 |
| HC(1-12)A8K12 (**P6**) | *Synthetic* | G | W | W | R | R | T | V | A | K | V | R | K |
| EeCentrocin 1 (**P1**)[1] | *E. esculentus* | G | W | W | R | R | T | V | D | K | V | R | N |
| SdCentrocin 1a HC[2] | *S. droebachiensis* | G | W | F | K | K | T | F | H | K | V | S | H |
| SdCentrocin 2 HC[2] | *S. droebachiensis* | S | W | F | S | R | T | V | H | N | V | G | N |
| XP_003727823[3] | *S. purpuratus* | S | W | F | S | R | A | V | H | K | V | S | H |
| XP_003727824[3] | *S. purpuratus* | S | W | F | S | R | A | A | H | K | V | S | H |
| XP_003730585[3] | *S. purpuratus* | G | W | F | K | H | A | F | H | H | V | T | H |
| XP_003724772[3] | *S. purpuratus* | S | W | F | T | D | A | F | K | K | V | S | K |

[1]Data obtained from Solstad *et al.*[15]

[2]Data obtained from Li *et al.*[14]

[3]Data and reference number obtained from NCBI.

**TABLE 3** Antibacterial activity (MIC in μM) of alanine scan peptides (**P8-P18**) derived from the lead peptide HC(1-12)A8K12 (**P6**). The interchangeable Ala-residues are shown in bold. The nomenclature depicts which amino acid has been exchanged with alanine (G1A: Gly1 is exchanged with Ala). The table also shows in-text number reference for each peptide, molecular weight (MW, g/mol), amino acid sequence, peptide net charge, and retention time (RT, min) on a RP-HPLC column

| | | | Amino acid sequence and position | | | | | | | | | | | | | | | Antibacterial activity, MIC (μM) | | | |
|---|---|---|---|---|---|---|---|---|---|---|---|---|---|---|---|---|---|---|---|---|---|
| No. | Peptide | MW | 1 | 2 | 3 | 4 | 5 | 6 | 7 | 8 | 9 | 10 | 11 | 12 | *C*-term | Charge | RT | Cg | Sa | Pa | Ec |
| **P8** | G1A | 1555.9 | **A** | W | W | R | R | T | V | A | K | V | R | K | -$NH_2$ | +6 | 5.3 | 0.8 | 25 | 6.3 | 12.5 |
| **P9** | W2A | 1426.7 | G | **A** | W | R | R | T | V | A | K | V | R | K | -$NH_2$ | +6 | 2.1 | 3.1 | 100 | 200 | 50 |
| **P10** | W3A | 1426.7 | G | W | **A** | R | R | T | V | A | K | V | R | K | -$NH_2$ | +6 | 2.2 | 0.8 | 25 | 100 | 100 |
| **P11** | R4A | 1456.7 | G | W | W | **A** | R | T | V | A | K | V | R | K | -$NH_2$ | +5 | 7.9 | 1.6 | 50 | 12.5 | 6.3 |
| **P12** | R5A | 1456.7 | G | W | W | R | **A** | T | V | A | K | V | R | K | -$NH_2$ | +5 | 7.3 | 0.8 | 100 | 25 | 6.3 |
| **P13** | T6A | 1511.8 | G | W | W | R | R | **A** | V | A | K | V | R | K | -$NH_2$ | +6 | 5.9 | 1.6 | 12.5 | 3.1 | 3.1 |
| **P14** | V7A | 1513.8 | G | W | W | R | R | T | **A** | A | K | V | R | K | -$NH_2$ | +6 | 4.0 | 1.6 | 100 | 12.5 | 12.5 |
| **P6** | HC(1-12)A8K12 | 1541.9 | G | W | W | R | R | T | V | **A** | K | V | R | K | -$NH_2$ | +6 | 5.2 | 0.4 | 12.5 | 1.6 | 3.1 |
| **P15** | K9A | 1484.8 | G | W | W | R | R | T | V | A | **A** | V | R | K | -$NH_2$ | +5 | 7.1 | 1.6 | 100 | 6.3 | 6.3 |
| **P16** | V10A | 1513.8 | G | W | W | R | R | T | V | A | K | **A** | R | K | -$NH_2$ | +6 | 4.1 | 1.6 | 100 | 6.3 | 12.5 |
| **P17** | R11A | 1456.7 | G | W | W | R | R | T | V | A | K | V | **A** | K | -$NH_2$ | +5 | 6.8 | 1.6 | 100 | 12.5 | 12.5 |
| **P18** | K12A | 1484.8 | G | W | W | R | R | T | V | A | K | V | R | **A** | -$NH_2$ | +5 | 6.9 | 0.8 | 50 | 6.3 | 6.3 |

and only two AMPs were antibacterial against *S. aureus* at 50 μg/ml concentrations; R4A (**P11**) and K12A (**P18**) (Table 3). The antibacterial profiles against the two Gram-negative strains were quite similar: the lead peptide HC(1-12)A8K12 (**P6**), T6A (**P13**), K9A (**P15**) and K12A (**P18**) were antibacterial at concentrations ≤6.3 μM, whereas W2A (**P9**) and W3A (**P10**) were the least antibacterial with MICs ≥50 μM against the Gram-negative bacterial strains (Table 3).

In general, all Ala-substitutions of the lead peptide HC(1-12)A8K12 (**P6**), except T6A (**P13**), resulted in reduced antibacterial activity (Table 3). This indicated that all residues except Thr6 (and perhaps Ala8) were of importance in **P6** to maintain optimal antibacterial activity. The peptide T6A (**P13**) was generally the second most potent AMP after **P6**. However, while T6A (**P13**) was only marginally less potent than the lead peptide against *S. aureus*, *P. aeruginosa*, and *E. coli*, a four-fold dilution separated T6A (**P13**) and **P6** against *C. glutamicum* (Table 3). This observation indicated a selective drop in the antibacterial activity of T6A (**P13**) against *C. glutamicum*. HC(1-12)A8K12 (**P6**) and T6A (**P13**) were different in that Thr is a polar residue without charge whereas Ala is a small hydrophobic residue. A helical wheel projection of the lead peptide HC(1-12)A8K12 (**P6**) (Figure 2B) shows that the polar residue (Thr6) is located on the hydrophobic face of a putative α-helix, potentially having an impact on the amphipathic character of the peptide. The three most potent peptides in the alanine scan, HC(1-12)A8K12 (**P6**), G1A (**P8**), and T6A (**P13**), had all medium hydrophobicity (as indicated by the retention times on RP-HPLC, Table 3), compared to the other peptides that were either more or less hydrophobic. Others also report a hydrophobicity-window for optimal antibacterial activity of AMPs.[30]

Replacement of the positively charged residues with Ala in R4A (**P11**), R5A (**P12**), K9A (**P15**), R11A (**P17**), and K12A (**P18**) resulted in 2-8-fold reduction of antibacterial activity against all strains tested (Table 3). This reduced activity can be explained by reduction of net positive charge of these peptides. A high net positive charge is shown to be important for cationic AMPs for the initial electrostatic interaction with bacterial cell membranes.[19,29] In addition, all the positively charged residues were in the hydrophilic and charged face of the proposed α-helix. Insertion of an additional hydrophobic residue in this region may therefore alter the amphipathic character of the peptide. Residue Lys12, which was positioned at the *C*-terminal end of the peptide, seemed to be the least important cationic residue according to the alanine scan experiment.

A noteworthy pair when considering individual amino acid substitutions were the Trp substitutions represented by the peptides W2A (**P9**) and W3A (**P10**) (Table 3). Trp is a bulky hydrophobic residue, commonly accepted as a contributor to antimicrobial activity in AMPs.[19,31] This was also apparent in the current alanine scan experiment, where replacement of the Trp-residues with Ala resulted in a dramatic loss of antibacterial activity. However, a few points can be made regarding the loss of antibacterial activity when these amino acids were replaced. The peptides W3A (**P10**) and G1A (**P8**) showed similar high potencies against the Gram-positive bacterial strains, but W3A (**P10**) was noticeably less potent than G1A (**P8**) against the Gram-negative bacterial strains (Table 3). The one AMP that was consistently least potent against all strains was W2A (**P9**), which indicate that Trp2 was a more important residue for antibacterial activity than Trp3 (Table 3). The exception being against *E. coli* where W2A (**P9**) was somewhat less potent than W3A (**P10**). As shown in Table 3, the retention times (hydrophobicity) on a C18 RP-HPLC column were reduced for W2A (**P9**) and W3A (**P10**) compared to the lead peptide HC(1-12)A8K12 (**P6**). This illustrates the importance of the hydrophobic character contributed by the two Trp-residues, which are located at the hydrophobic face of the predicted α-helix (Figure 2B). Increased hydrophobicity of the hydrophobic face of an amphipathic peptide generally increases antimicrobial activity.[32]

Replacement of the polar uncharged Gly1 with a small hydrophobic Ala-residue (G1A, **P8**) resulted in 2-4-fold reduced antibacterial activity against all the strains compared to the lead peptide HC(1-12)A8K12 (**P6**) (Table 3). In the helical wheel projection of **P6** (Figure 2B), Gly1 is positioned in the polar and cationic face of the predicted α-helix. Insertion of a hydrophobic residue in this position will affect the amphipathic character of the peptide (also demonstrated by a slight increase in retention time; Table 3), resulting in decreased activity. In addition, Gly does not have a side chain and may therefore provide increased flexibility to this region of the peptide. The results support the previous notion on the importance of *N*-terminal Gly in AMPs.[17]

Ala-substitution of the hydrophobic Val7 in V7A (**P14**) or Val10 in V10A (**P16**), both positioned in the hydrophobic face of the predicted α-helix (Figure 2B), resulted in 4-8-fold decrease in activity against all bacterial strains tested (Table 3). Val contains an isopropyl side chain, in contrast to the methyl side chain in Ala. Replacement of Val with Ala would therefore slightly alter the hydrophobicity in the hydrophobic sector and thereby the overall amphipathicity of the peptide, an important characteristic of AMPs.[4] As shown in Table 3, the retention times were reduced for V7A (**P14**) and V10A (**P16**), indicating reduced hydrophobicity for these two peptides compared to the lead peptide HC(1-12)A8K12 (**P6**).

### 3.3 | Bacterial killing experiments

On the basis of our SAR studies (Tables 1 and 3), the peptide HC(1-12)A8K12 (**P6**) was the most effective peptide at inhibiting bacterial growth. We therefore performed bacterial killing experiments on *E. coli* and *S. aureus*, to evaluate if the peptide displayed bacteriostatic or bactericidal properties. The results suggest that HC(1-12)A8K12 (**P6**) exhibited bactericidal properties against both bacterial strains at MIC, as no CFU were detected after plating of cultures treated with minimal inhibitory (or higher) concentrations of the peptide (Figure 3). On the other hand, treatment with sub-MIC concentrations of the peptide produced >$10^8$ CFU/mL for both strains after 24 h of incubation.

### 3.4 | Antifungal activity

The synthesised peptides were subjected to antifungal screening against the moulds *A. pullulans* and *Rhodotorula* sp., and the yeast *C.*

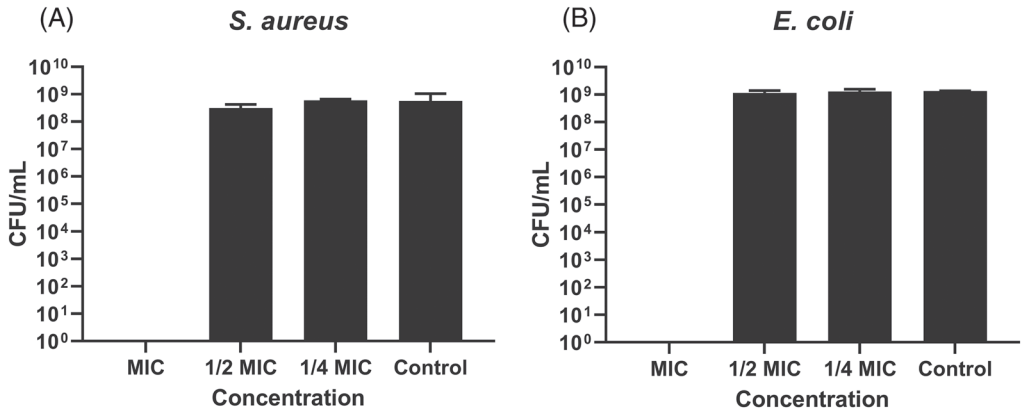


**FIGURE 3** Bactericidal activity of HC(1-12)A8K12 (**P6**). Colony-forming units (CFU/mL) were counted from *S. aureus* (MIC=12.5 μM) and *E. coli* (MIC=3.1 μM) treated with MIC and sub-MIC concentrations (½ x MIC and ¼ x MIC) of **P6**. The mean of three replicates ± SD is displayed.

*albicans*. The lead peptide HC(1-12)A8K12 (**P6**) was superior in activity compared to the other peptides, including the full HC (**P1**) peptide (Table 4). The lead peptide (**P6**) was antifungal at concentrations ranging from 3.1-12.5 μM, whereas the other peptides had antifungal MICs from 12.5 μM and higher. All the 12-residue alanine scan peptides (except the lead peptide HC(1-12)A8K12, **P6**) displayed antifungal activity at concentrations ranging from 12.5-50 μM (Table 4). In addition, whereas the full HC (**P1**) peptide was more potent against bacteria than fungi, the lead peptide HC(1-12)A8K12 (**P6**) was equally potent against both types of microorganisms, i.e. showing broad-spectrum antimicrobial activity. By comparison, fluconazole displayed a MIC value of 50 μM against *C. albicans* and a MIC of 25 μM against *A. pullulans*. Fluconazole was inactive (MIC>100 μM) against *Rhodotorula* sp.

## 3.5 | Haemolytic and cytotoxic activity

The lead peptide HC(1-12)A8K12 (**P6**) and a selection of the other synthetic peptides were screened for haemolytic activity against

**TABLE 4** Antifungal (MIC in μM), haemolytic (% haemolysis at 200 μM and 25 μM), and cytotoxic activities ($IC_{50}$ in μM) of EeCentrocin 1 HC (**P1**), truncated and modified analogues (**P2**-**P4** and **P6**) and alanine scan peptides (**P8**-**P18**)

| | | Antifungal activity (MIC, μM) | | | Haemolytic activity (RBC haemolysis, %) | | Cytotoxic activity ($IC_{50}$, μM) | |
|---|---|---|---|---|---|---|---|---|
| No. | Peptide | *C. albicans* | *A. pullulans* | *Rhodotorula* sp. | 200 μM | 25 μM | A2058 | MRC-5 |
| **P1** | HC[1] | 100 | 12.5 | 12.5 | 74.6 | 13.5 | 56 | 125 |
| **P2** | HC(1-16) | 100 | 50 | 25 | 0 | 0 | >200 | >200 |
| **P3** | HC(1-16)A8 | Nt[2] | Nt | Nt | 5.0 | 0 | >200 | >200 |
| **P4** | HC(2-16)A7 | 100 | >100 | 100 | Nt | Nt | Nt | Nt |
| **P8** | G1A | 25 | 50 | 12.5 | 1.6 | 0 | >100[3] | >100[3] |
| **P9** | W2A | 50 | 50 | 25 | 0 | 0 | >200 | >200 |
| **P10** | W3A | 50 | 50 | 25 | 0 | 0 | >200 | >200 |
| **P11** | R4A | 25 | 50 | 50 | 3.6 | 0 | >200 | >200 |
| **P12** | R5A | 25 | 25 | 12.5 | 0 | 0 | >200 | >200 |
| **P13** | T6A | 25 | 25 | 12.5 | 4.1 | 0.9 | Nt | Nt |
| **P14** | V7A | 25 | 25 | 12.5 | 0 | 0 | >200 | >200 |
| **P6** | HC(1-12)A8K12 | 6.3 | 12.5 | 3.1 | 25.1 | 2.4 | >200 | >200 |
| **P15** | K9A | 25 | 25 | 12.5 | 5.1 | 0 | >200 | >200 |
| **P16** | V10A | 25 | 50 | 12.5 | 1 | 0 | Nt | Nt |
| **P17** | R11A | 25 | 50 | 12.5 | 0 | 0 | >200 | >200 |
| **P18** | K12A | 25 | 50 | 12.5 | 0 | 0 | Nt | Nt |

[1]Antifungal data of EeCentrocin 1 HC (**P1**) are derived from Solstad *et al.* [15]

[2]Nt = Not tested.

[3]Highest concentration tested.

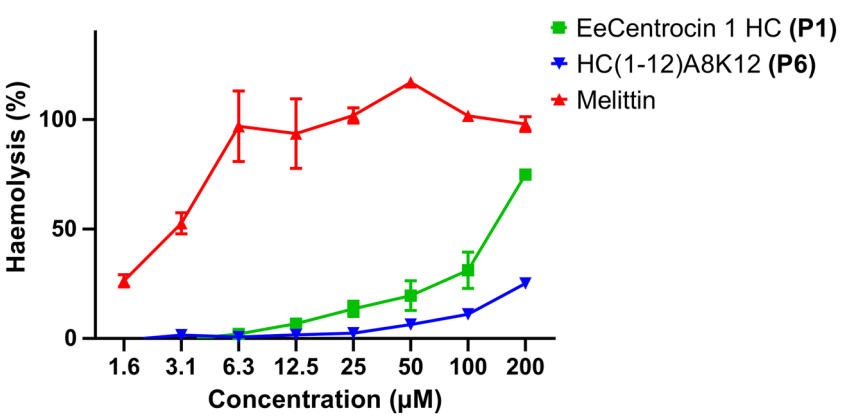


**FIGURE 4** Haemolytic activity (% haemolysis) against human red blood cells of EeCentrocin 1 HC (**P1**), the lead peptide HC(1-12)A8K12 (**P6**), and the bee venom, melittin.

human red blood cells and for cytotoxic activity against human melanoma (A2058) and fibroblast (MRC-5) cell lines. The results obtained indicated a correlation between antibacterial and haemolytic activity (Table 4). The peptides showing highest haemolytic activity were the lead peptide HC(1-12)A8K12 (**P6**) and the full HC (**P1**) peptide. Thus, **P6** showed 25% haemolysis at 200 μM, and **P1** showed 75% haemolysis at 200 μM (Table 4 and Figure 4). At concentrations closer to the MIC-values, the haemolytic activity of **P6** was negligible. All the other peptides displayed minor (<5%) or no haemolytic activity at 200 μM. By contrast, the bee venom peptide, melittin, displayed 100% haemolysis at concentrations as low as 6.3 μM (Figure 4). Only EeCentrocin 1 HC (**P1**) displayed cytotoxic activity at the concentrations tested, having $IC_{50}$ values of 56 μM against human melanoma cells (A2058) and 125 μM against human fibroblast cells (MRC-5) (Table 4).

## 4 | CONCLUSIONS

Pathogenic bacteria are becoming resistant to most antibiotics to an ever-increasing extent. This has spurred the discovery of novel antibacterial compounds such as AMPs isolated from natural sources. Such natural bioactive peptides are promising templates for designing shorter analogues with retained or even improved therapeutic potential. Truncation of the heavy chain (**P1**) of the marine antimicrobial peptide EeCentrocin 1, and selected amino acid substitutions, combined with *C*-terminal amidation, led to a 12-residue lead peptide with potent antibacterial and antifungal activities. This lead peptide HC(1-12)A8K12 (**P6**) contains five cationic residues and five non-polar residues, and is possibly forming an amphipathic α-helical structure when interacting with bacterial membranes, as suggested by helical wheel projections and secondary structure predictions. An alanine-scan experiment revealed that most of the amino acids present in the identified lead peptide HC(1-12)A8K12 (**P6**) were crucial for maintaining maximum activity, indicating that the peptide has a highly ordered amphipathic structure with well-separated hydrophobic and cationic regions. The peptide displayed potent antifungal activity and low haemolytic and cytotoxic activity at MIC concentrations, making it a promising lead peptide for further drug development.

## ACKNOWLEDGEMENTS

The study was supported by the Biotek 2021 programme of the Research Council of Norway, project XBioPepS (grant No. 208546). The authors appreciate the technical assistance given by Hege Devold and Kirsti Helland (both UiT) regarding bioactivity assays, and the help provided by Jack-Ansgar Bruun and Toril Anne Grønset (both UiT) regarding MS-analysis.

## ORCID

*Runar G. Solstad* https://orcid.org/0000-0003-3463-6034
*Klara Stensvåg* https://orcid.org/0000-0002-4717-6711
*Morten B. Strøm* https://orcid.org/0000-0003-1973-0778
*Tor Haug* https://orcid.org/0000-0003-1104-5813

## REFERENCES

1. Boucher HW, Talbot GH, Bradley JS, et al. Bad bugs, no drugs: no eskape! An update from the Infectious Diseases Society of America. *Clin Infect Dis*. 2009;48(1):1-12.
2. Zasloff M. Antimicrobial peptides of multicellular organisms. *Nature*. 2002;415(6870):389-395.
3. Brogden KA. Antimicrobial peptides: pore formers or metabolic inhibitors in bacteria? *Nat Rev Microbiol*. 2005;3(3):238-250.
4. Bahar AA, Ren D. Antimicrobial peptides. *Pharmaceuticals*. 2013;6(12):1543-1575.
5. Peschel A, Sahl H-G. The co-evolution of host cationic antimicrobial peptides and microbial resistance. *Nat Rev Microbiol*. 2006;4(7):529-536.
6. Hancock REW, Lehrer R. Cationic peptides: a new source of antibiotics. *Trends Biotechnol*. 1998;16(2):82-88.
7. Nguyen LT, Haney EF, Vogel HJ. The expanding scope of antimicrobial peptide structures and their modes of action. *Trends Biotechnol*. 2011;29(9):464-472.
8. Lázár V, Martins A, Spohn R, et al. Antibiotic-resistant bacteria show widespread collateral sensitivity to antimicrobial peptides. *Nat Microbiol*. 2018;3(6):718-731.
9. Bechinger B, Gorr S-U. Antimicrobial peptides: mechanisms of action and resistance. *J Dent Res*. 2017;96(3):254-260.
10. Fox JL. Antimicrobial peptides stage a comeback. *Nat Biotechnol*. 2013;31(5):379-382.
11. Zasloff M. Antimicrobial peptides: do they have a future as therapeutics? In: Harder J, Schröder J-M, eds. *Antimicrob. Pept*. Cham: Springer International Publishing; 2016:147-154.

12. Molchanova N, Hansen P, Franzyk H. Advances in development of antimicrobial peptidomimetics as potential drugs. *Molecules*. 2017;22:1430.
13. Mahlapuu M, Håkansson J, Ringstad L, Björn C. Antimicrobial peptides: an emerging category of therapeutic agents. *Front Cell Infect Microbiol*. 2016;6:194.
14. Li C, Haug T, Moe MK, Styrvold OB, Stensvåg K. Centrocins: Isolation and characterization of novel dimeric antimicrobial peptides from the green sea urchin, *Strongylocentrotus droebachiensis*. *Dev Comp Immunol*. 2010;34(9):959-968.
15. Solstad RG, Li C, Isaksson J, et al. Novel antimicrobial peptides EeCentrocins 1, 2 and EeStrongylocin 2 from the edible sea urchin *Echinus esculentus* have 6-Br-Trp post-translational modifications. *PLoS ONE*. 2016;11:e0151820.
16. Sodergren E, Weinstock GM, Davidson EH, et al. The genome of the sea urchin *Strongylocentrotus purpuratus*. *Science*. 2006;314(5801):941-952.
17. Tossi A, Sandri L, Giangaspero A. Amphipathic, α-helical antimicrobial peptides. *Biopolymers*. 2000;55(1):4-30.
18. Schibli DJ, Epand RF, Vogel HJ, Epand RM. Tryptophan-rich antimicrobial peptides: comparative properties and membrane interactions. *Biochem Cell Biol*. 2002;80(5):667-677.
19. Chan DI, Prenner EJ, Vogel HJ. Tryptophan- and arginine-rich antimicrobial peptides: structures and mechanisms of action. *Biochim Biophys Acta, Biomembr*. 2006;1758:1184-1202.
20. Sperstad SV, Haug T, Vasskog T, Stensvåg K. Hyastatin, a glycine-rich multi-domain antimicrobial peptide isolated from the spider crab (*Hyas araneus*) hemocytes. *Mol Immunol*. 2009;46(13):2604-2612.
21. Sperstad SV, Haug T, Paulsen V, et al. Characterization of crustins from the hemocytes of the spider crab, *Hyas araneus*, and the red king crab, *Paralithodes camtschaticus*. *Dev Comp Immunol*. 2009;33(4):583-591.
22. Hansen KØ, Isaksson J, Bayer A, Johansen JA, Andersen JH, Hansen E. Securamine derivatives from the Arctic bryozoan *Securiflustra securifrons*. *J Nat Prod*. 2017;80(12):3276-3283.
23. Montgomerie S, Cruz JA, Shrivastava S, Arndt D, Berjanskii M, Wishart DS. PROTEUS2: a web server for comprehensive protein structure prediction and structure-based annotation. *Nucleic Acids Res*. 2008;36(Web Server issue):W202-W209.
24. Lamiable A, Thévenet P, Rey J, Vavrusa M, Derreumaux P, Tufféry P. PEP-FOLD3: faster *de novo* structure prediction for linear peptides in solution and in complex. *Nucleic Acids Res*. 2016;44(W1):W449-W454.
25. Zhang Z, Schwartz S, Wagner L, Miller W. A greedy algorithm for aligning DNA sequences. *J Comput Biol*. 2000;7(1-2):203-214.
26. Jiang Z, Vasil AI, Hale JD, Hancock RE, Vasil ML, Hodges RS. Effects of net charge and the number of positively charged residues on the biological activity of amphipathic α-helical cationic antimicrobial peptides. *Biopolymers*. 2008;90(3):369-383.
27. Shalev DE, Mor A, Kustanovich I. Structural consequences of carboxyamidation of Dermaseptin S3. *Biochemistry*. 2002;41(23):7312-7317.
28. Dolling R, Beyermann M, Haenel J, et al. Piperidine-mediated side product formation for Asp (OBut)-containing peptides. *J Chem Soc Chem Commun*. 1994;7:853-854.
29. Takahashi D, Shukla SK, Prakash O, Zhang G. Structural determinants of host defense peptides for antimicrobial activity and target cell selectivity. *Biochimie*. 2010;92:1236-1241.
30. Chen Y, Guarnieri MT, Vasil AI, Vasil ML, Mant CT, Hodges RS. Role of peptide hydrophobicity in the mechanism of action of α-helical antimicrobial peptides. *Antimicrob Agents Chemother*. 2007;51(4):1398-1406.
31. Strøm MB, Haug BE, Skar ML, et al. The pharmacophore of short cationic antibacterial peptides. *J Med Chem*. 2003;46:1567-1570.
32. Huang Y, Huang J, Chen Y. Alpha-helical cationic antimicrobial peptides: relationships of structure and function. *Protein Cell*. 2010;1(2):143-152.

## SUPPORTING INFORMATION

Additional supporting information may be found online in the Supporting Information section at the end of the article.

**How to cite this article:** Solstad RG, Johansen C, Stensvåg K, Strøm MB, Haug T. Structure-activity relationship studies of shortened analogues of the antimicrobial peptide EeCentrocin 1 from the sea urchin *Echinus esculentus*. *J Pep Sci*. 2019; e3233. https://doi.org/10.1002/psc.3233